THE RESIDUAL CAPACITY ESTIMATION OF FULLY SEALED 25 A h LEAD/ACID CELLS

M. HUGHES, R. T. BARTON, S. A. G. R. KARUNATHILAKA and N. A. HAMPSON

Department of Chemistry, University of Technology, Loughborough, Leics. LE11 3TU (U.K.)

R. LEEK

Department of Electrical and Electronic Engineering, University of Technology, Loughborough, Leics. LE11 3TU (U.K.)

(Received June 26, 1985; in revised form November 26, 1985)

Summary

Impedance measurements on large, 25 A h, spiral-wound, fully sealed lead/acid cells in the frequency range 60 kHz - 1 mHz are discussed. A residual capacity test parameter, which seems to be independent of cycle number, discharge rate, and age of the cell, and which can also be used to indicate the state-of-health of such cells, has been identified.

Introduction

The introduction of the fully sealed technology into battery manufacture has created another problem in the estimation of the residual capacity of such systems. In flooded cells, specific gravity measurements coupled to open circuit voltage measurements could give some indication of the residual capacity. In fully sealed cells, the only measurable parameter is the cell voltage. Because of this, impedance investigations of cells were carried out, as it was believed that such measurements would provide the most useful data.

The large capacity 25 A h cells proved to have low impedances. We have already established procedures for measuring low impedances (in the Ni–Cd systems [1, 2]) and these were applied to the impedance measurements of the lead/acid cell. Studies of the fully sealed 2.5 A h lead/acid cell [3] had revealed the effectiveness of using the impedance analogue technique for estimating the residual capacity of such cells. The hope was that the parameters isolated for the lower capacity cell would hold equally well for the larger capacity cells. The results of our investigations are considered below.

0378-7753/86/$3.50

Experimental

A five-year old 12 V aircraft battery of 25 A h capacity at the 10 hour rate, and 18 A h capacity at the 1 hour rate, was first investigated. After cycling, charging at 1.8 A for 18 h, and discharging at the 1 hour rate (18 A), the battery could deliver more than the nominal battery capacity and was considered adequate for the experiments. After an open circuit stand period of three months, the battery was dismantled and each cell cycled. The cells were discharged at the one hour rate to an end voltage of 1.67 V and then recharged at 1.8 A for 14 h. During this cycling period most of the cells showed an anomalous behaviour and, as a result, the impedance behaviour of brand new cells was compared with that of old cells which still showed a satisfactory behaviour on cycling.

The new cells were discharged in a similar manner to the old cells but were charged under a modified, constant potential procedure. This involved four stages: charging at 10 A until the cell reached 2.3 V, then reducing the current to 5 A until 2.3 V was regained; next, 1 A was maintained until the voltage reached 2.35 V and, finally, charging was completed at a constant 2.35 V until the current fell to a minimum (about 3 or 4 mA) and remained constant for at least 2 h.

The cells were discharged at 18 A or 36 A until the required state-of-charge was reached. After a 1 h equilibration period the impedance spectrum was recorded. The true cell capacity was determined by discharging the cell to 1.67 V at 18 A or 1.59 V at 36 A.

The impedance measurement equipment was a frequency response analyser coupled to a microcomputer data logger/data analyser. The data were transferred to a mainframe computer for subsequent analysis.

Results and discussion

1. Anomalous behaviour of the 25 A h lead/acid cells ex 12 V aircraft battery

Mention has already been made of the anomalous behaviour of the older cells on cycling. The impedance spectra of the cells represent such erratic behaviour as:

(i) the potential of the cell dropping to zero volts on open circuit after accepting charge;

(ii) venting;

(iii) becoming full of gas with an on-charge voltage exceeding 8.7 V.

These, Figs. 2 - 4, are compared with the spectra of a normal cell, Fig. 1.

The behaviour of cells which vented or which had an on-charge voltage over 8.7 V when only partially charged, is disturbing. Normally O_2 (produced at the positive electrode) recombines with the H_2 at the negative electrode, but in these cells it could not cope with the oxygen and, hence, the gases built up inside the cell. The reason for the inability of the electrode

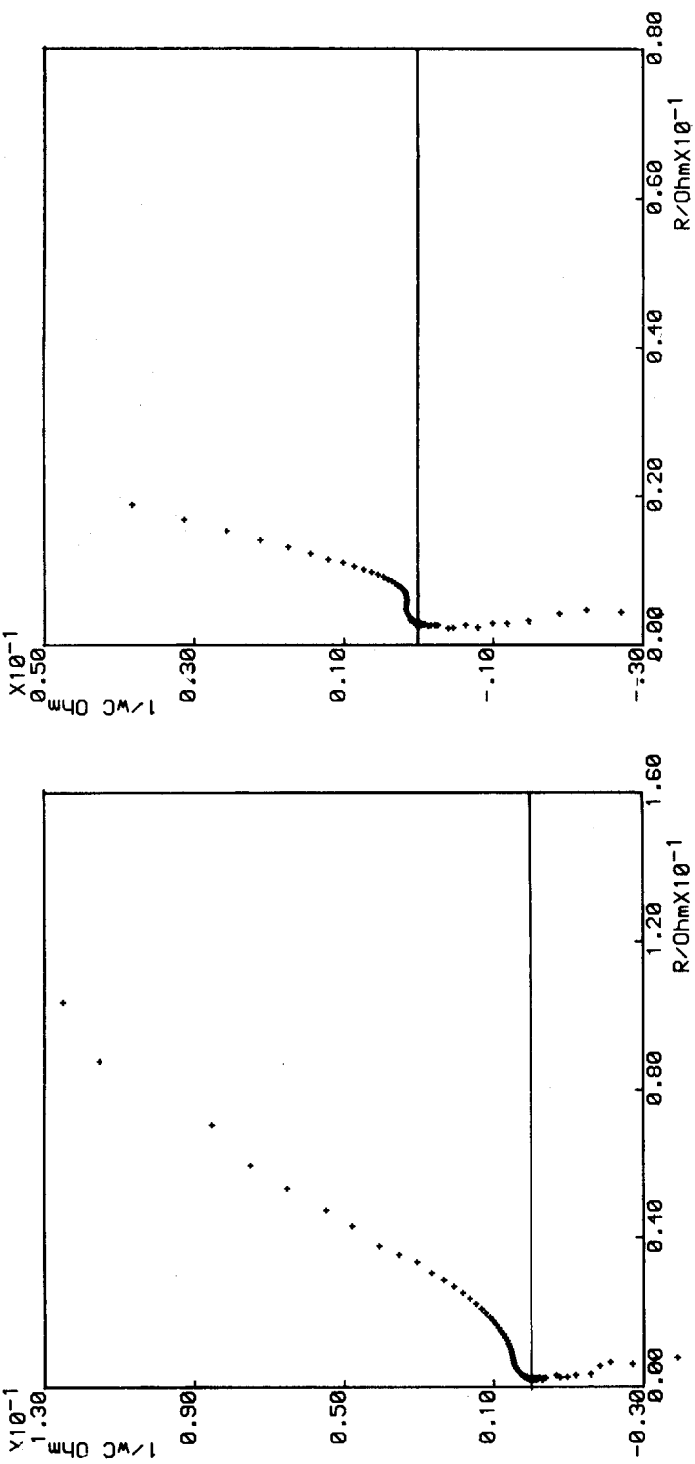

Fig. 1. Impedance spectrum of a fully sealed, 5-year old 25 A h Pb/acid cell (ex 12 V 25 A h battery) 100% charged, which behaved normally on cycling. Spectrum taken after its second cycle in the frequency range 60 kHz - 0.6 mHz. Ten points per decade.

Fig. 2. As Fig. 1 but for a cell which showed the presence of films. Measurements in the frequency range 60 kHz - 2 mHz.

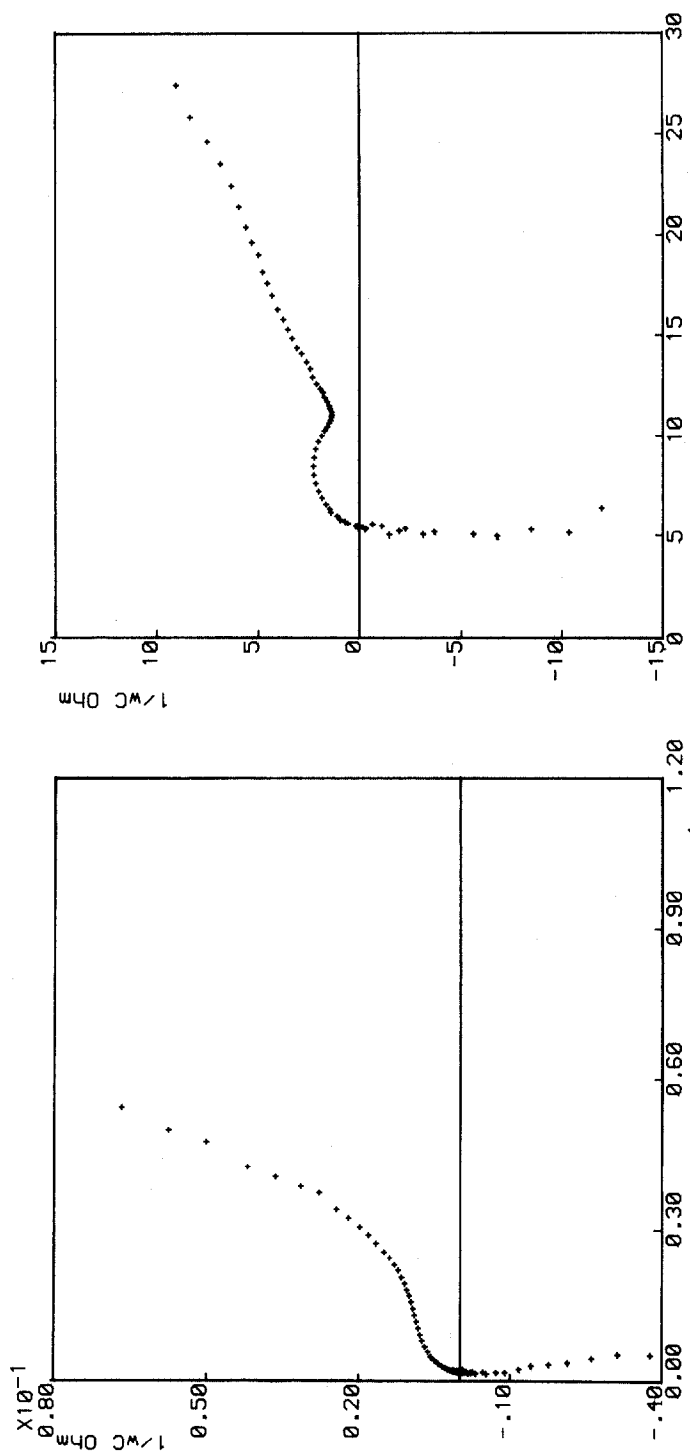

Fig. 3. As Fig. 1 but for a cell whose voltage fell to 0.0 V on open circuit voltage. Measurements in the frequency range 60 kHz - 2 mHz.

Fig. 4. As Fig. 1 but for a cell which became full of gas. Measurements in the frequency range 60 kHz - 2 mHz.

to cope with the oxygen evolution so early on in the charging process is not yet understood.

Only the impedance spectra of cells which became full of gas and which could not deliver their rated capacity show peculiarities. In the latter case, Fig. 2 shows a high dihedral (slope, $(1/\omega CR)$) at low frequencies (high $1/\omega C$) which indicates the presence of a dielectric — probably $PbSO_4$ — which cannot be broken down on cycling. Figure 4 shows the impedance spectrum of the cell which filled with gas. Of note is the dihedral which the loci make at low frequencies, which is only 22½°. This indicates a system having semi-infinite porous electrodes, which is obviously the result of the gases under pressure.

The cells received a prolonged open circuit stand period of approximately three months early on in their history. This aspect of the operation of "Cyclon" cells seems to be significant, especially as 2.5 A h cells [3] which were left standing for approximately seven years could deliver their rated capacity after cycling for a few times only. This difference could be the result of use of phosphoric acid in the older cells [4] which is known to limit the growth of $PbSO_4$ crystals.

The results of the impedance estimations of these cells are representative of others which fall into roughly the same behavioural groups. The results in themselves are qualitatively important for they show that measurements such as the present ones are capable of reflecting the factors which affect the battery state-of-health. The correlation of frequency responses with behavioural patterns is an important aspect of our work and will be the subject of later papers.

2. Variation of the impedance spectra with the residual capacity of the cells

As the impedance spectra of the remaining old cells and the new cells are practically identical at similar states-of-charge and at the two discharge rates, only the impedance spectra from one of the new cells discharged at the C rate shall be shown.

In general, the results for the larger capacity 25 A h cells paralleled those of the 2.5 A h cells, giving confidence that we have obtained the true impedance of the larger capacity cells, as expected from introducing our computer correction to the cell impedance. This result would be expected since the smaller cells contained similar grids with the same thickness of active material as the larger cells. The impedance spectra of the cell over the complete states-of-charge range are presented as Sluyters and Randles plots in Figs. 5 - 14.

Figure 5 is the Sluyters plot of a fully charged cell. The spectrum, although representing a complex system, is simple. At high frequencies the most prominent feature is a small inductive arc which, on an equivalent circuit, resembles an inductor shunted by a parallel resistor. This type of self-inductance has already been observed in cells [5 - 7] and may be attributed qualitatively to the geometrical arrangement of the electrodes and the conductors within the cell. At lower frequencies, the cell impedance becomes

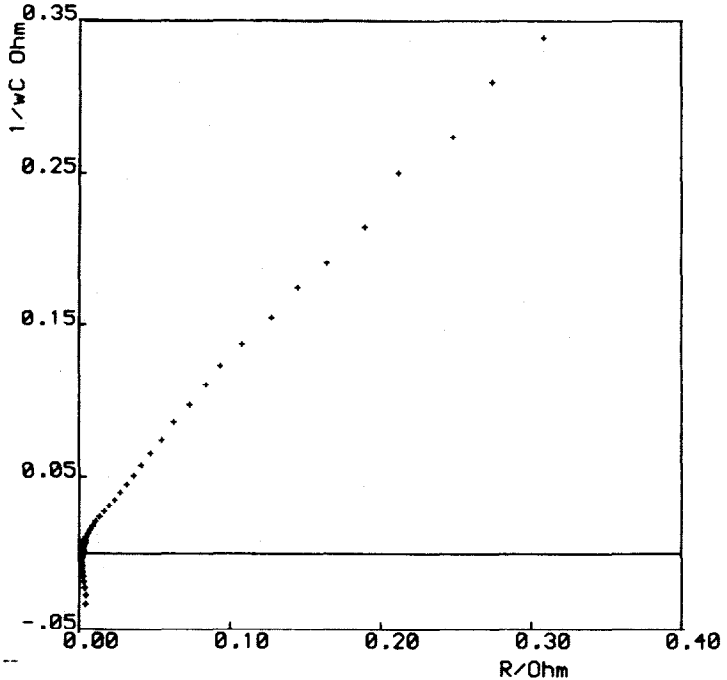

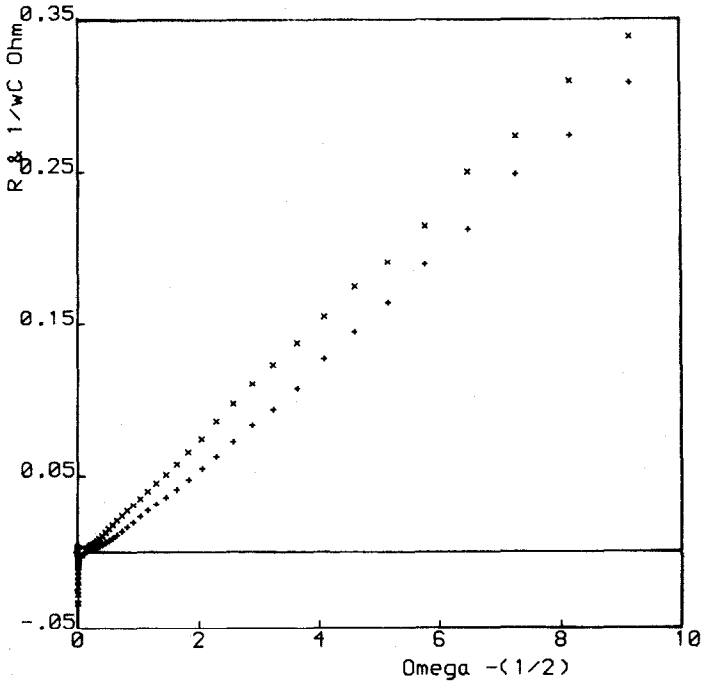

Fig. 5. Impedance spectrum of a new, fully-sealed 25 A h Pb/acid cell 100% charged in the frequency range 60 kHz - 0.6 mHz. Ten points per decade.

Fig. 6. Randles representation of a new, fully-sealed 25 A h Pb/acid cell 100% charged. +, R; ×, $1/\omega C$.

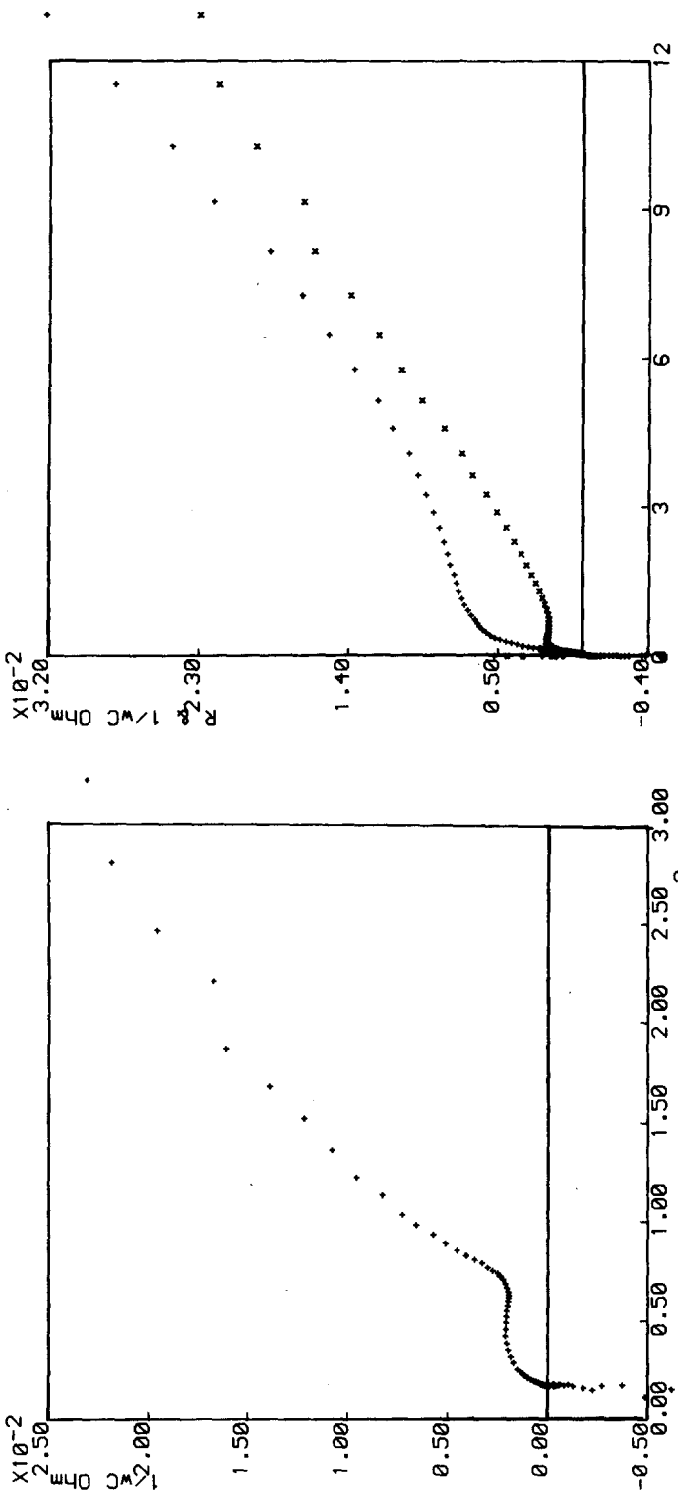

Fig. 7. Impedance spectrum of a new, fully-sealed 25 A h Pb/acid cell, 90% state-of-charge, in the frequency range 60 kHz - 0.3 mHz. Ten points per decade.

Fig. 8. Randles representation of a new, fully-sealed 25 A h Pb/acid cell 90% charged. +, R; ×, $1/\omega C$.

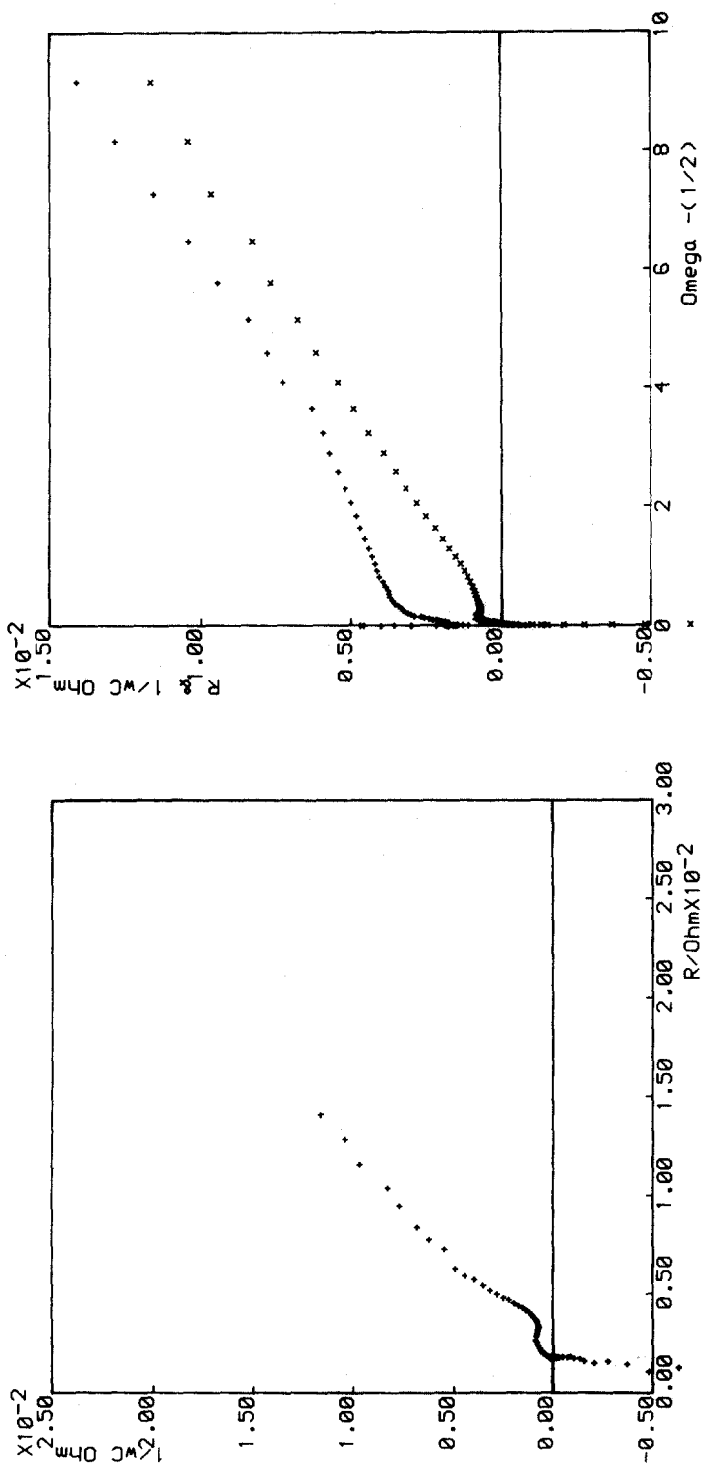

Fig. 9. Impedance plot of a new, fully-sealed 25 A h Pb/acid cell 60% charged in the frequency range 60 kHz - 0.6 mHz. Ten points per decade.

Fig. 10. Randles representation of a fully-sealed 25 A h Pb/acid cell 60% charged. +, R; ×, $1/\omega C$.

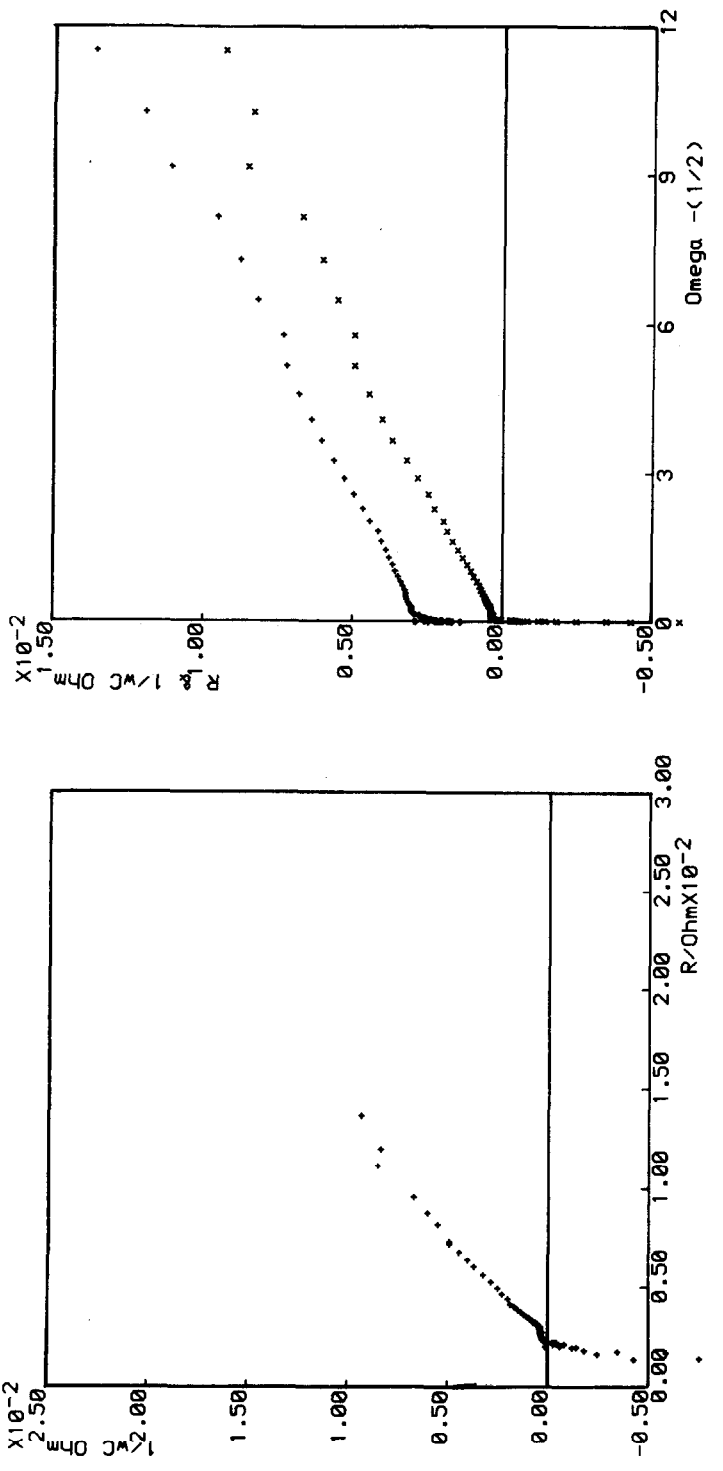

Fig. 11. Impedance plot of a new, fully-sealed 25 A h Pb/acid cell 20% charged in the frequency range 60 kHz - 0.3 mHz. Ten points per decade.

Fig. 12. Randles representation of a new, fully-sealed 25 A h Pb/acid cell 20% charged. +, R; ×, $1/\omega C$.

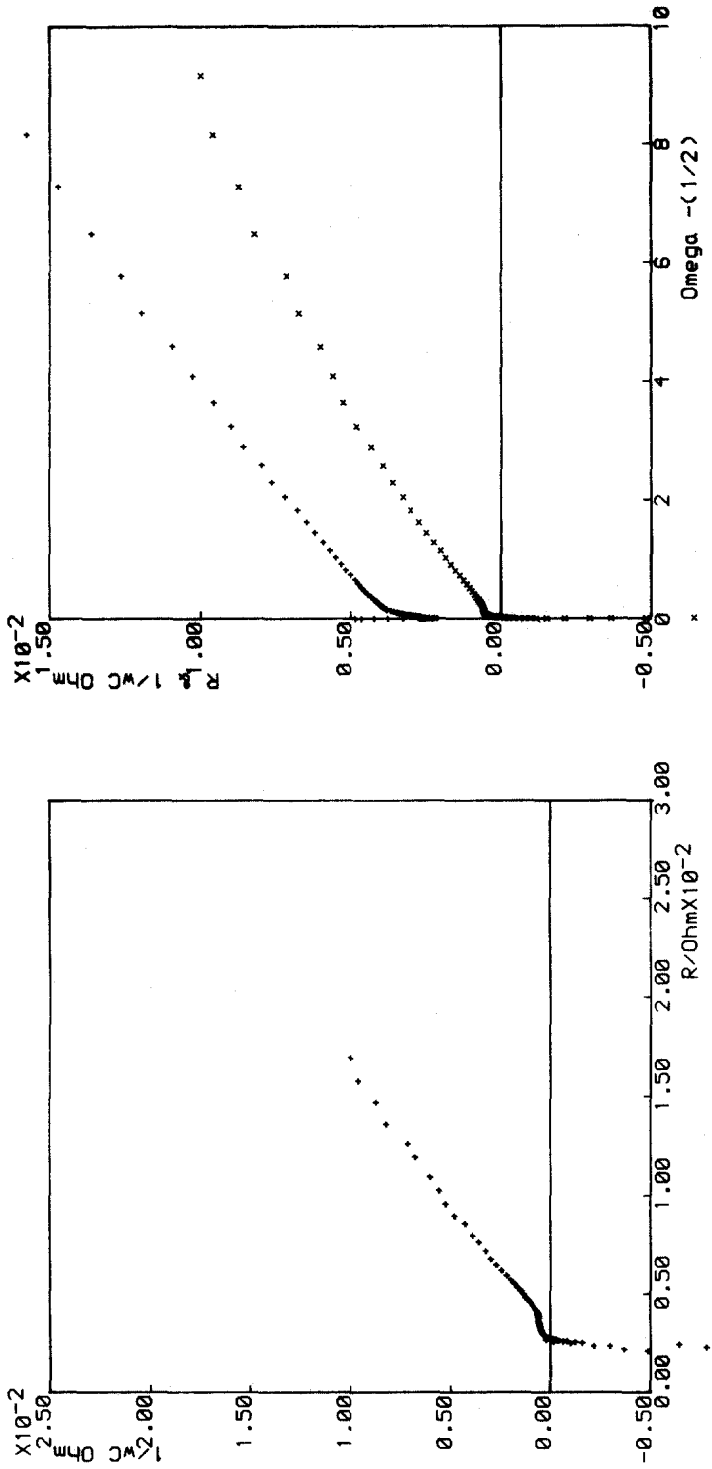

Fig. 13. Impedance plot of a new, fully-sealed 25 A h Pb/acid cell 0% charged in the frequency range 60 kHz - 0.6 mHz. Ten points per decade.

Fig. 14. Randles representation of a new, fully-sealed 25 A h Pb/acid cell 0% charged. +, R; ×, $1/\omega C$.

capacitive and the spectrum develops into a distorted semi-circle which rapidly relaxes into a further shape in which the loci subtend an angle of 55° to the real axis. The magnitude of the capacitive reactance at low frequencies is predominant. It seems likely that this results largely from the concentration polarisation which depends on the diffusional and transport properties within the cell. Work by Keddam *et al.* [5] supports this view. They showed that the impedance of fully charged negative plates at frequencies below 1 Hz behaved similarly to that arising from a Nernst diffusion layer of finite thickness. In the case of a fully sealed lead/acid cell, the mass transport properties would be expected to be important, particularly if the cell was discharged, since the cell would be operating in an electrolyte starved mode. The high dihedral at low frequencies indicates the presence of an additional capacitative term which is clearly observed in the Randles plot, Fig. 6. This shows the resistive component lying below the capacitive component, which is indicative of adsorption.

Figure 7 is an impedance plot of a cell containing 90% residual capacity. It shows the presence of a well developed, high frequency semi-circle which relaxes into a Warburg tail in which the loci subtend an angle of initially 58° and then 45° to the real axis at lower frequencies.

At intermediate and lower states-of-charge, the impedance spectra follow the trends established in the 90% charged cell. As can be seen, the only differences in the Sluyters plots, Figs. 7, 9, 11, 13, are in the magnitudes of the high frequency semi-circle which decrease to about 30% state-of-charge, and then begin to broaden in the last 20% of charge. The changes in the dihedral angle at low frequencies are maintained throughout the remaining states-of-charge, which show that the electrodes are behaving as planar electrodes. The Randles plots of the intermediate states-of-charge, Figs. 8, 10, 12, 14, clearly indicate the absence of blocking films which might have been expected to be present. The impedance data were matched to the same analogue circuit as was used for the 2.5 A h cells and are shown in Fig. 15.

In all cases the decomposition was satisfactorily accomplished, and Tables 1 - 4 show the values of the circuit elements corresponding to the various residual capacities of the old and new cells discharged at the 1 and 2 *C* rates. Only in the new cells and at low frequencies do any deficiencies in

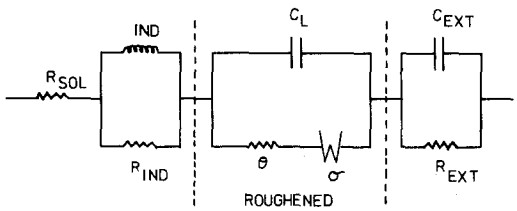

Fig. 15. Analogue circuit used to describe the impedance of the fully-sealed 25 A h Pb/acid cell in the frequency range 60 kHz - 1 mHz.

TABLE 1

Values of computed circuit components for a new 25 A h cell discharged at the *C* rate

Residual capacity (%)		R_{Sol} (Ω)	θ (Ω)	C_L (F)	σ ($\Omega\ s^{-1/2}$)	γ	C_{EXT} (F)	R_{EXT} (Ω)	IND (H)	R_{IND} (Ω)	Error (±)
1.23	R	2.72 E^{-3}	3.22 E^{-4}	18.26	7.01 E^{-4}	0.85	5.27 E^{8+}	1 E^{12+}	9.63 E^{-8+}	0.55	3.46 E^{-5}
	C	2.72 E^{-3+}	2.04 E^{-4}	23.93	6.07 E^{-4}	0.81	5.27 E^{8}	1 E^{12+}	9.63 E^{-8}	0.55+	2.54 E^{-5}
13.46	R	2.34 E^{-3}	1.18 E^{-4}	85.47	2.16 E^{-4}	0.76	2.48 E^{4}	0.10	9.36 E^{-8+}	1 E^{12+}	7.69 E^{-5}
	C	2.34 E^{-E+}	1.23 E^{-6}	1.11 E^{4}	4.65 E^{-6}	0.5+	5995	7.87	9.36 E^{-8}	1 E^{12+}	1.36 E^{-4}
21.85	R	2.25 E^{-3}	6.89 E^{-5}	167.1	7.55 E^{-5}	0.75	6465+	2.51 E^{-3}	9.43 E^{-8+}	3.17	1.08 E^{-4}
	C	2.25 E^{-3+}	4.90 E^{-5}	210.1	6.03 E^{-5}	0.71	6465	6.39 E^{-3}	9.43 E^{-8}	3.17+	1.93 E^{-4}
32.46	R	1.75 E^{-3}	2.33 E^{-4}	16.06	3.84 E^{-4}	0.91	8100+	1.90 E^{-2}	9.79 E^{-8+}	1.02	1.47 E^{-4}
	C	1.75 E^{-3+}	5.43 E^{-6}	601.6	2.79 E^{-5}	0.64	8100	5.78 E^{-3}	9.79 E^{-8}	1.02+	1.61 E^{-4}
40.35	R	1.87 E^{-3}	7.14 E^{-4}	24.99	4.74 E^{-4}	0.86	1.21 E^{4}	2.15 E^{-3}	8.50 E^{-8+}	0.58	6.03 E^{-5}
	C	1.87 E^{-3+}	4.14 E^{-4}	44.85	3.91 E^{-4}	0.79	9458	4.59 E^{-3}	8.50 E^{-8}	0.58+	7.07 E^{-5}
50.82	R	1.77 E^{-3}	7.91 E^{-4}	9.835	8.92 E^{-4}	1.0+	3.55 E^{5}	5.68 E^{-6}	8.55 E^{-8+}	1.25	1.10 E^{-4}
	C	1.77 E^{-3+}	1.22 E^{-4}	85.46	2.31 E^{-4}	0.80	1.21 E^{4}	2.58 E^{-3}	8.55 E^{-8}	1.25+	2.85 E^{-5}
63.33	R	1.80 E^{-3}	8.59 E^{-4}	18.90	6.64 E^{-4}	0.92	10005+	1 E^{12+}	9.80 E^{-8+}	0.38	3.14 E^{-5}
	C	1.80 E^{-3+}	3.13 E^{-4}	59.73	3.26 E^{-4}	0.80	10005	1 E^{12+}	9.80 E^{-8}	0.38+	2.42 E^{-5}
71.81	R	1.64 E^{-3}	3.48 E^{-4}	68.99	2.47 E^{-4}	0.79	5995+	1.64 E^{-2}	9.00 E^{-8+}	0.45	1.05 E^{-4}
	C	1.64 E^{-3+}	2.05 E^{-4}	110.4	2.22 E^{-4}	0.74	5995	9.42 E^{-3}	9.00 E^{-8}	0.45	9.08 E^{-5}
80.53	R	1.68 E^{-3}	1.89 E^{-3}	20.40	7.79 E^{-4}	0.90	4807+	1.28 E^{-2}	1.16 E^{-7+}	0.24	7.23 E^{-4}
	C	1.68 E^{-3+}	1.04 E^{-3}	42.09	7.03 E^{-4}	0.81	4807	1.28 E^{-2+}	1.16 E^{-7}	0.24	1.32 E^{-4}
90.36	R	1.72 E^{-3}	8.67 E^{-4}	85.23	2.60 E^{-4}	0.77	8614+	5.45 E^{-3}	9.50 E^{-8+}	0.32	1.60 E^{-4}
	C	1.72 E^{-3+}	6.15 E^{-4}	113.2	3.51 E^{-4}	0.73	8614	1.73 E^{-2}	9.50 E^{-8}	0.32+	5.43 E^{-5}
100	R	1.86 E^{-3}	1.76 E^{-2}	13.90	2.90 E^{-2}	1.0+	612.8	5.30 E^{-2}	9.50 E^{-8+}	0.41	1.06 E^{-3}
	C	1.86 E^{-3+}	2.49 E^{-2}	9.77	3.11 E^{-2}	1.0+	651.2	9.20 E^{-2}	9.50 E^{-8}	0.41+	2.49 E^{-3}

Notes to tables

(1) R denotes computation made using resistive values; (2) C denotes computation made using capacitative values; (3) Circuit components defined by Fig. 15; specifically: R_{sol} denotes solution resistance; C_{EXT}, R_{EXT} — external capacitance/resistance parallel element; θ denotes charge-transfer resistance; IND, R_{IND} — cell inductive parallel element; σ Warburg coefficient; γ Roughness factor; (4) + denotes value bounded ±10% in the computation.

TABLE 2

Values of computed circuit components for an old 25 A h cell discharged at the 2 C rate

Residual capacity (%)		R_{Sol} (Ω)	θ (Ω)	C_L (F)	σ ($\Omega\ s^{-1/2}$)	γ	C_{EXT} (F)	R_{EXT} (Ω)	IND (H)	R_{IND} (Ω)	Error (±)
19.53	R	2.49 E^{-3}	8.14 E^{-7}	1.46 E^{4}	4.20 E^{-4}	0.5^{+}	1 E$^{12^{+}}$	1.23 E^{-3}	8.56 E^{-8}	0.10	5.96 E^{-4}
	C	2.49 E$^{-3^{+}}$	1.06 E^{-6}	2.10 E^{4}	7.70 E^{-4}	0.5^{+}	1 E$^{12^{+}}$	7.11 E^{-3}	7.94 E^{-8}	0.10^{+}	3.87 E^{-4}
11.87	R	2.73 E^{-3}	3.17 E^{-4}	66.44	6.01 E^{-4}	0.93	8 E$^{4^{+}}$	5.64 E^{-3}	7.37 E^{-8}	0.10	4.78 E^{-4}
	C	2.73 E$^{-3^{+}}$	1.28 E^{-4}	204.5	2.62 E^{-4}	0.79	8 E$^{4^{+}}$	9.71 E^{-3}	1.14 E^{-7}	5.10 E^{-2}	9.41 E^{-4}
8.66	R	2.60 E^{-3}	2.10 E^{-4}	64.86	4.35 E^{-4}	0.87	1 E$^{12^{+}}$	1.95 E^{-3}	7.41 E^{-8}	2.25 E^{-2}	1.61 E^{-4}
	C	2.60 E$^{-3^{+}}$	1.02 E^{-4}	193.0	2.34 E^{-4}	0.78	1 E$^{12^{+}}$	1.95 E$^{-3^{+}}$	1.14 E^{-7}	5.10 E^{-2}	1.50 E^{-4}
1.76	R	2.96 E^{-3}	9.23 E^{-5}	37.19	4.16 E^{-4}	0.79	1999	1.75 E^{-5}	1.04 E$^{-7^{+}}$	0.32	2.29 E^{-4}
	C	2.96 E$^{-3^{+}}$	3.36 E^{-5}	195.3	2.44 E^{-4}	0.73	5284	2.38 E^{-3}	1.04 E^{-7}	0.32^{+}	2.18 E^{-4}
31.11	R	2.85 E^{-3}	4.22 E^{-4}	8.16	1.80 E^{-5}	1.0^{+}	39965^{+}	1 E$^{12^{+}}$	1.19 E$^{-7^{+}}$	0.26	1.54 E^{-4}
	C	2.85 E$^{-3^{+}}$	3.98 E^{-4}	15.00	1.14 E^{-5}	1.0^{+}	40000	1 E$^{12^{+}}$	1.19 E^{-7}	0.26^{+}	1.57 E^{-4}
39.03	R	2.67 E^{-3}	9.24 E^{-4}	6.77	1.25 E^{-1}	1.0^{+}	7435	2.62 E^{-3}	1.19 E$^{-7^{+}}$	0.18^{+}	6.80 E^{-5}
	C	2.67 E$^{-3^{+}}$	2.99 E^{-4}	26.51	7.68 E^{-4}	0.86	6946	2.34 E^{-3}	1.19 E^{-7}	0.18	6.05 E^{-5}
53.72	R	2.50 E^{-3}	3.77 E^{-4}	33.21	4.40 E^{-4}	0.85	3980	4.20 E^{-3}	1.06 E$^{-7^{+}}$	0.27	1.00 E^{-4}
	C	2.50 E$^{-3^{+}}$	7.11 E^{-4}	13.72	1.28 E^{-3}	0.95	7534	1.06 E^{-3}	1.06 E^{-7}	0.27^{+}	6.06 E^{-5}
61.3	R	2.43 E^{-3}	1.16 E^{-4}	193.1	1.74 E^{-4}	0.67	1667	1.05 E^{-2}	1.12 E$^{-7^{+}}$	0.17	7.68 E^{-5}
	C	2.43 E$^{-3^{+}}$	1.40 E^{-4}	164.9	2.93 E^{-4}	0.68	2152	2.29 E^{-2}	1.12 E^{-7}	0.17^{+}	6.61 E^{-5}
88.8	R	1.96 E^{-3}	1.51 E^{-3}	5.37	1.23 E^{-3}	1.0^{+}	4832^{+}	7.70 E^{-3}	1.27 E$^{-7^{+}}$	0.24	6.75 E^{-4}
	C	1.96 E$^{-3^{+}}$	1.50 E^{-3}	10.23	1.32 E^{-3}	1.0^{+}	4832	7.70 E$^{-3^{+}}$	1.27 E^{-7}	0.11	6.24 E^{-4}
83.93	R	1.99 E^{-3}	1.22 E^{-4}	206.8	1.70 E^{-4}	0.71	5000^{+}	1.69 E^{-2}	1.00 E$^{-7^{+}}$	6.19 E^{-2}	7.05 E^{-5}
	C	1.99 E$^{-3^{+}}$	7.51 E^{-5}	134.5	2.39 E^{-4}	0.71	5000	1.79 E^{-2}	1.00 E^{-7}	6.19 E^{-2}	6.62 E^{-5}
100	R	1.87 E^{-3}	5.96 E^{-4}	578.0	1.02 E^{-3}	0.60	5816	1 E$^{12^{+}}$	1.14 E$^{-7^{+}}$	0.30	9.81 E^{-5}
	C	1.87 E$^{-3^{+}}$	6.50 E^{-4}	571.6	1.00 E^{-3}	0.60	3421	1 E$^{12^{+}}$	1.14 E^{-7}	0.30^{+}	1.13 E^{-4}

TABLE 3

Values of computed circuit components for an old 25 A h cell discharged at the 1 *C* rate

Residual capacity (%)		R_{Sol} (Ω)	θ (Ω)	C_L (F)	σ ($\Omega\ s^{-1/2}$)	γ	C_{EXT} (F)	R_{EXT} (Ω)	IND (H)	R_{IND} (Ω)	Error (±)
1.3	R	2.14 E^{-3}	8.16 E^{-5}	248.7	1.16 E^{-4}	0.69	3958	1.10 E^{-2}	1.04 E^{-7+}	5.45 E^{-2}	8.36 E^{-5}
	C	2.14 E^{-3+}	1.25 E^{-3}	13.79	1.18 E^{-4}	0.98	3161	1.59 E^{-2}	1.04 E^{-7}	5.45 E^{-2+}	1.14 E^{-4}
10.0	R	2.26 E^{-3}	9.75 E^{-5}	196.4	2.86 E^{-4}	0.81	5959	7.43 E^{-3}	1.03 E^{-7+}	4.59 E^{-2}	9.45 E^{-5}
	C	2.26 E^{-3+}	8.34 E^{-4}	19.17	3.47 E^{-4}	1.0^{+}	3120	1.47 E^{-2}	1.03 E^{-7}	4.59 E^{-2+}	1.06 E^{-4}
22.48	R	2.49 E^{-3}	9.56 E^{-5}	106.1	4.54 E^{-4}	0.90	6.78 E^{4}	5.01 E^{-5}	1.00 E^{-7+}	6.92 E^{-2}	7.32 E^{-5}
	C	2.49 E^{-3+}	9.68 E^{-5}	99.58	4.24 E^{-4}	0.90	7870	7.96 E^{-4}	1.00 E^{-7}	6.92 E^{-2+}	5.79 E^{-5}
27.63	R	2.52 E^{-3}	1.36 E^{-4}	16.69	1.36 E^{-3}	0.99	1889	6.38 E^{-4}	1.10 E^{-7+}	5.68 E^{-3}	3.45 E^{-4}
	C	2.52 E^{-3+}	1.29 E^{-4}	17.62	8.94 E^{-4}	1.0^{+}	3901	6.38 E^{-4+}	1.10 E^{-7}	3.00 E^{-2}	2.76 E^{-4}
43.16	R	2.22 E^{-3}	2.58 E^{-4}	58.27	5.16 E^{-4}	0.91	4446	9.01 E^{-3}	8.34 E^{-8+}	5.80 E^{-2}	3.78 E^{-5}
	C	2.22 E^{-3+}	8.50 E^{-5}	266.7	5.20 E^{-4}	0.79	4989	2.54 E^{-3}	8.34 E^{-8}	5.80 E^{-2+}	4.35 E^{-5}
47.60	R	2.00 E^{-3}	3.45 E^{-5}	98.52	3.80 E^{-4}	0.83	9516	3.70 E^{-3}	8.11 E^{-8+}	5.38 E^{-2}	2.81 E^{-4}
	C	2.00 E^{-3+}	1.25 E^{-4}	12.65	1.19 E^{-3}	1.0^{+}	1.15 E^{4}	2.12 E^{-3}	8.11 E^{-8}	5.38 E^{-2+}	4.85 E^{-5}
61.17	R	2.06 E^{-3}	1.09 E^{-4}	10.86	1.31 E^{-3}	1.0^{+}	1 E^{12+}	3.17 E^{-3}	8.24 E^{-8+}	4.67 E^{-2}	1.75 E^{-4}
	C	2.06 E^{-3+}	8.16 E^{-5}	13.23	1.56 E^{-3}	1.0^{+}	1 E^{12+}	3.17 E^{-3+}	8.24 E^{-8}	4.67 E^{-2+}	1.20 E^{-4}
71.66	R	2.01 E^{-3}	5.92 E^{-5}	334.3	9.17 E^{-5}	0.70	3160^{+}	1.38 E^{-2}	9.61 E^{-8+}	4.59 E^{-2}	6.26 E^{-4}
	C	2.01 E^{-3+}	2.25 E^{-5}	892.6	4.88 E^{-5}	0.63	3160	1.38 E^{-2+}	9.61 E^{-8}	4.59 E^{-2+}	4.13 E^{-4}
79.88	R	2.14 E^{-3}	8.16 E^{-5}	248.7	1.16 E^{-4}	0.69	3958	1.10 E^{-2}	1.04 E^{-7+}	3.91 E^{-2}	9.45 E^{-5}
	C	2.14 E^{-3+}	1.25 E^{-3}	13.79	1.18 E^{-4}	0.98	3161	1.10 E^{-2+}	1.04 E^{-7}	5.45 E^{-2}	7.05 E^{-5}
90.05	R	1.99 E^{-3}	1.27 E^{-3}	9.68	2.03 E^{-3}	1.0^{+}	2775^{+}	3.92 E^{-2}	1.06 E^{-7+}	0.30	6.20 E^{-4}
	C	1.99 E^{-3+}	8.81 E^{-5}	453.8	1.09 E^{-4}	0.66	2775	3.92 E^{-2+}	1.06 E^{-7}	0.30^{+}	6.52 E^{-4}
100	R	2.06 E^{-3}	1.74 E^{-3}	102.0	1.26 E^{-3}	0.74	3000	1 E^{6+}	1.15 E^{-7+}	0.18	1.47 E^{-4}
	C	2.06 E^{-3+}	8.52 E^{-3}	15.84	4.42 E^{-3}	1.0^{+}	6617	1 E^{6+}	1.15 E^{-7}	0.18^{+}	3.43 E^{-4}

TABLE 4

Values of computed circuit components for a new 25 A h cell discharged at the 2 C rate

Residual capacity (%)		R_{Sol} (Ω)	θ (Ω)	C_L (F)	σ ($\Omega\ s^{-1/2}$)	γ	C_{EXT} (F)	R_{EXT} (Ω)	IND (H)	R_{IND} (Ω)	Error ($\pm$)
6.18	R	2.34 E^{-3}	4.82 E^{-4}	14.19	8.10 E^{-4}	0.92	1.52 E^{4}	1.52 E^{-2}	9.52 E^{-8+}	1.64	5.88 E^{-5}
	C	2.34 E^{-3+}	1.00 E^{-4}	58.09	2.49 E^{-4}	0.76	1.52 E^{4}	7.32 E^{-3}	9.52 E^{-8}	1.64^{+}	1.23 E^{-4}
13.46	R	1.50 E^{-3}	9.48 E^{-4}	15.5	6.95 E^{-4}	0.97	5268	2.95 E^{-3}	9.44 E^{-8+}	2.83 E^{4}	1.69 E^{-4}
	C	1.50 E^{-3+}	9.25 E^{-4}	9.94	1.23 E^{-3}	1.0^{+}	1.68 E^{4}	8.45 E^{-4}	9.44 E^{-8}	2.83 E^{4+}	5.26 E^{-4}
20.50	R	9.80 E^{-4}	2.18 E^{-6}	3641	6.51 E^{-6}	0.63	1.76 E^{4}	2.89 E^{-3}	5.95 E^{-8+}	7.75 E^{10}	8.87 E^{-5}
	C	9.80 E^{-4+}	3.22 E^{-6}	1871	6.58 E^{-6}	0.63	1.41 E^{4}	5.86 E^{-3}	5.95 E^{-8}	7.75 E^{10}	2.28 E^{-4}
43.09	R	1.11 E^{-3}	3.66 E^{-5}	216.5	6.10 E^{-5}	0.80	7891	2.20 E^{-3}	5.87 E^{-8+}	1.86 E^{5}	7.33 E^{-5}
	C	1.11 E^{-3+}	5.44 E^{-5}	153.9	7.12 E^{-5}	0.80	9599	4.38 E^{-3}	5.87 E^{-8}	1.86 E^{5+}	1.16 E^{-4}
43.17	R	1.22 E^{-3}	2.34 E^{-4}	23.75	8.19 E^{-6}	1.0^{+}	9468	3.19 E^{-3}	6.19 E^{-8}	5.97 E^{6}	3.21 E^{-5}
	C	1.22 E^{-3+}	2.86 E^{-4}	7.12	7.19 E^{-6}	1.0^{+}	5716	5.41 E^{-3}	6.19 E^{-8}	5.97 E^{6}	3.26 E^{-5}
50.16	R	1.57 E^{-3}	4.38 E^{-4}	30.35	2.51 E^{-4}	0.91	5390	1.68 E^{-3}	7.78 E^{-8+}	5.9	2.59 E^{-4}
	C	1.57 E^{-3+}	4.96 E^{-4}	28.64	3.99 E^{-4}	0.91	1.36 E^{4}	5.50 E^{-3}	7.78 E^{-8}	5.9^{+}	2.24 E^{-4}
66.46	R	1.53 E^{-3}	1.27 E^{-3}	17.88	9.20 E^{-4}	0.94	9206	4.96 E^{-3}	8.02 E^{-8+}	2.05 E^{4}	7.86 E^{-5}
	C	1.53 E^{-3+}	9.32 E^{-4}	19.24	1.21 E^{-3}	0.91	9837	3.86 E^{-3}	8.02 E^{-8}	2.05 E^{4+}	1.38 E^{-4}
74.9	R	1.20 E^{-3}	7.66 E^{-4}	16.88	2.96 E^{-4}	1.0^{+}	3629	4.23 E^{-3}	8.16 E^{-8}	8.67 E^{8}	1.69 E^{-4}
	C	1.20 E^{-3+}	7.34 E^{-4}	16.4	9.12 E^{-4}	1.0^{+}	4.52 E^{4}	2.08 E^{-3}	8.16 E^{-8}	8.67 E^{8+}	1.16 E^{-4}
83.6	R	1.55 E^{-3}	9.68 E^{-4}	43.05	5.77 E^{-4}	0.85	5010	5.78 E^{-3}	1.05 E^{-7+}	0.65	1.02 E^{-4}
	C	1.55 E^{-3+}	7.13 E^{-4}	58.73	6.46 E^{-4}	0.82	5759	1.57 E^{-2}	1.05 E^{-7}	0.65^{+}	1.57 E^{-4}
93.26	R	1.35 E^{-3}	1.98 E^{-3}	73.38	5.98 E^{-4}	0.82	1.17 E^{4}	3.09 E^{-3}	8.90 E^{-8+}	2.24 E^{7}	5.58 E^{-5}
	C	1.35 E^{-3+}	1.14 E^{-3}	63.35	9.46 E^{-4}	0.83	1.36 E^{4}	9.68 E^{-3}	8.90 E^{-8}	2.24 E^{7+}	4.78 E^{-5}
100	R	1.55 E^{-3}	6.29 E^{-2}	206.3	9.66 E^{-3}	0.64	5822	1.32 E^{-2}	1.06 E^{-7+}	0.36	1.20 E^{-3}
	C	1.55 E^{-3+}	0.11	190.5	9.26 E^{-3}	0.61	5849	1.34 E^{-2}	1.06 E^{-7}	0.36^{+}	8.49 E^{-4}

our model become apparent. That this is only observed in the new cells might indicate that the diffusional process inside these new cells does not come to an equilibrium within a limited cycle period. The computer matches of the Sluyters and Randles plots for the new cell discharged at the *C* rate are shown in Figs. 16 - 21, where the continuous curves represent the computer matches, and the points the experimental data.

Taking the results together, it seems that the extra capacitance in the Randles plot of the fully charged cell is a result of gassing; possibly oxygen in solution or in the gas phase or combined with the negative electrode as outlined below.

$$Pb + \tfrac{1}{2}O_2 + H_2SO_4 \longrightarrow PbSO_4 + H_2O$$

This could explain why the extra capacitance is only observed in the fully charged cell.

The changes observed in the Warburg tail are also of interest. The final slope throughout the complete states-of-charge is always ~45°, which indicates that the electrodes are behaving as planar electrodes at all charge states. The computed value of the roughness factor (γ) shows it to remain practically constant around 0.9. Because there is no effective change in γ as charge is withdrawn from the cell, this indicates that $PbSO_4$ is continuously produced at the surface rather than within the obviously porous matrix. When the cell is fully charged, the pore size must be large in relation to the reaction layer, and can sustain a discharge at the *C* and 2 *C* rates at the surface of the electrodes only. At high current densities any reaction inside the pores would be very short lived because the acid would not readily be replaced by diffusion.

These results are apparently at variance with those of the 2.5 A h cells, which clearly show that, as the cell is discharged, the electrodes become more porous in nature and may be treated as electrodes having semi-infinite pores when completely discharged. In this case the current densities are very much lower and, as a result, as the cell is discharged, the reaction can be driven further into the body of the electrode with no subsequent electrolyte starvation.

In our analogue circuit we have considered both electrodes as having similar impedances. It is possible that when the cell is fully charged the impedances of the two electrodes are sufficiently different to cause a change in the expected impedance plot (from a simple Randles circuit). This could result in the observed Warburg tail leaving the high frequency semi-circle at an initial angle of about 55°. When the cell is discharged, both electrodes become 'coated' with $PbSO_4$ which causes their impedances to be practically identical. This is observed in the impedance spectrum of the fully discharged cell which shows the Warburg tail subtending only one angle of 45° to the real axis. The effect of the second electrode in our analogue circuit is represented by the external capacitor shunted by the resistor. At low states-of-charge, the charge-transfer resistance again begins to increase. This is

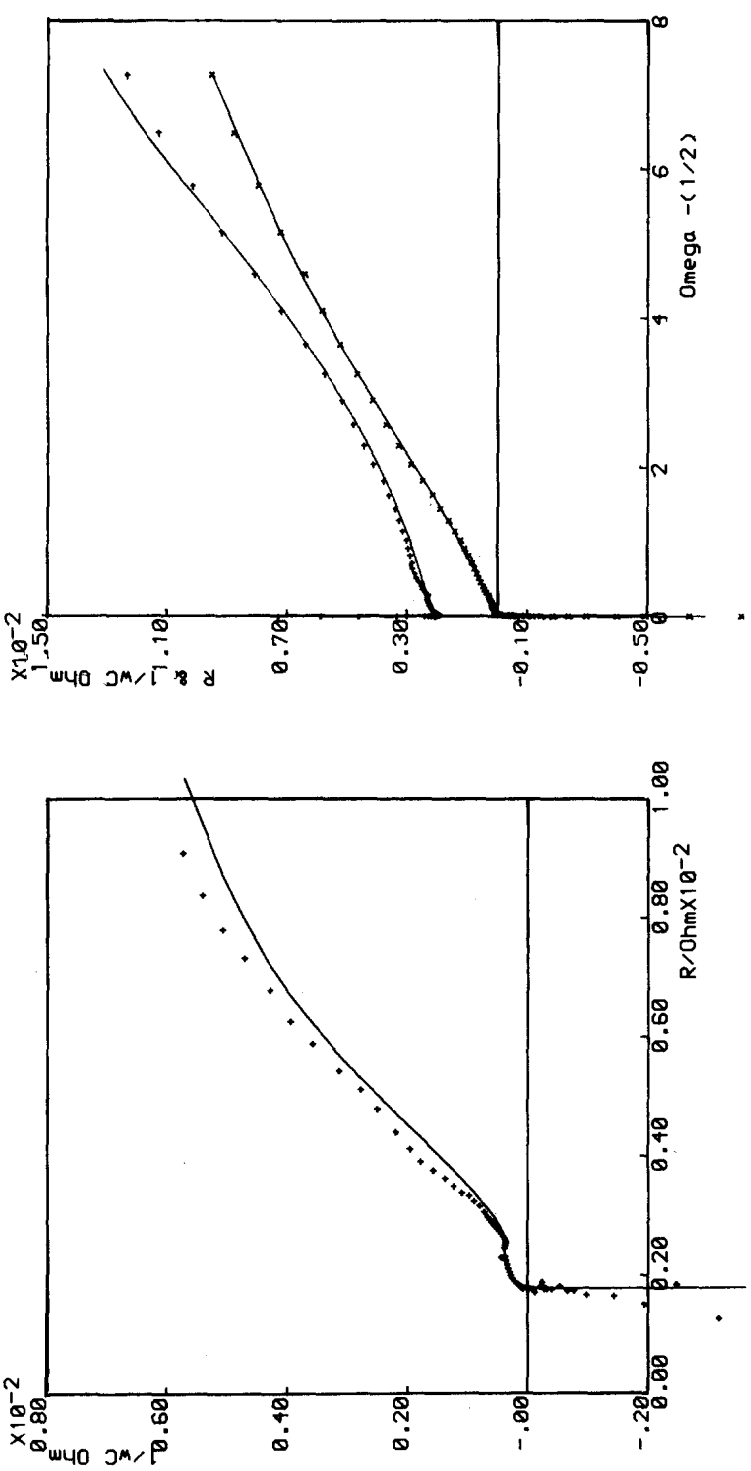

Fig. 16. Sluyters plot of the results of the computer fit for the fully-sealed 25 A h Pb/acid cell 80% charged in the frequency range 60 kHz - 40 mHz.

Fig. 17. Randles representation of the results of the computer fit for the fully-sealed 25 A h Pb/acid cell 80% charged. +, R; ×, $1/\omega C$.

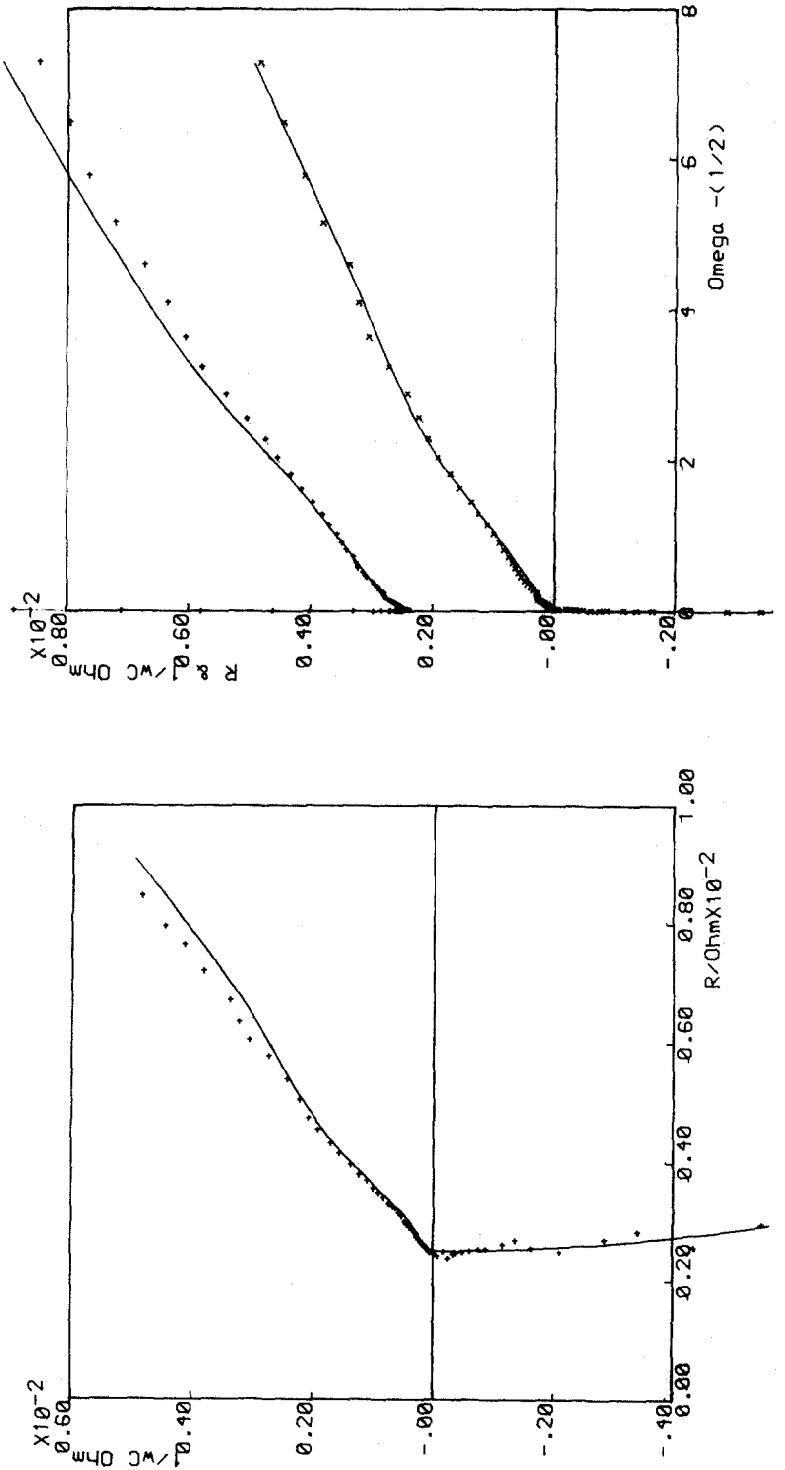

Fig. 18. Sluyters plot of the results of the computer fit for the fully-sealed 25 A h Pb/acid cell, 50% charged, in the frequency range 60 kHz - 40 mHz.

Fig. 19. Randles representation of the results of the computer fit for the fully-sealed 25 A h Pb/acid cell 50% charged. +, R; ×, $1/\omega C$.

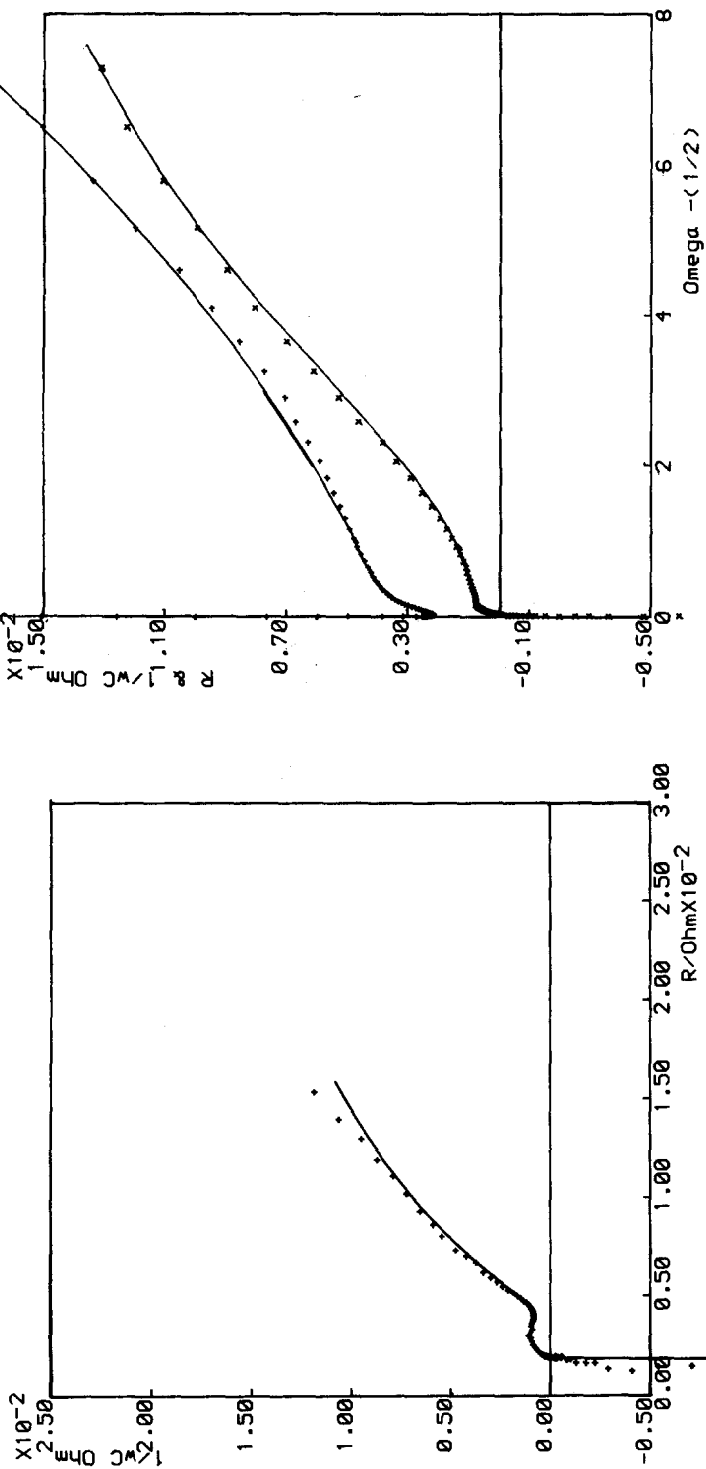

Fig. 20. Sluyters plot of the results of the computer fit for the fully-sealed 25 A h Pb/acid cell, 20% charged, in the frequency range 60 kHz - 40 mHz.

Fig. 21. Randles representation of the results of the computer fit for the fully-sealed 25 A h Pb/acid cell 20% charged. +, R; ×, $1/\omega C$.

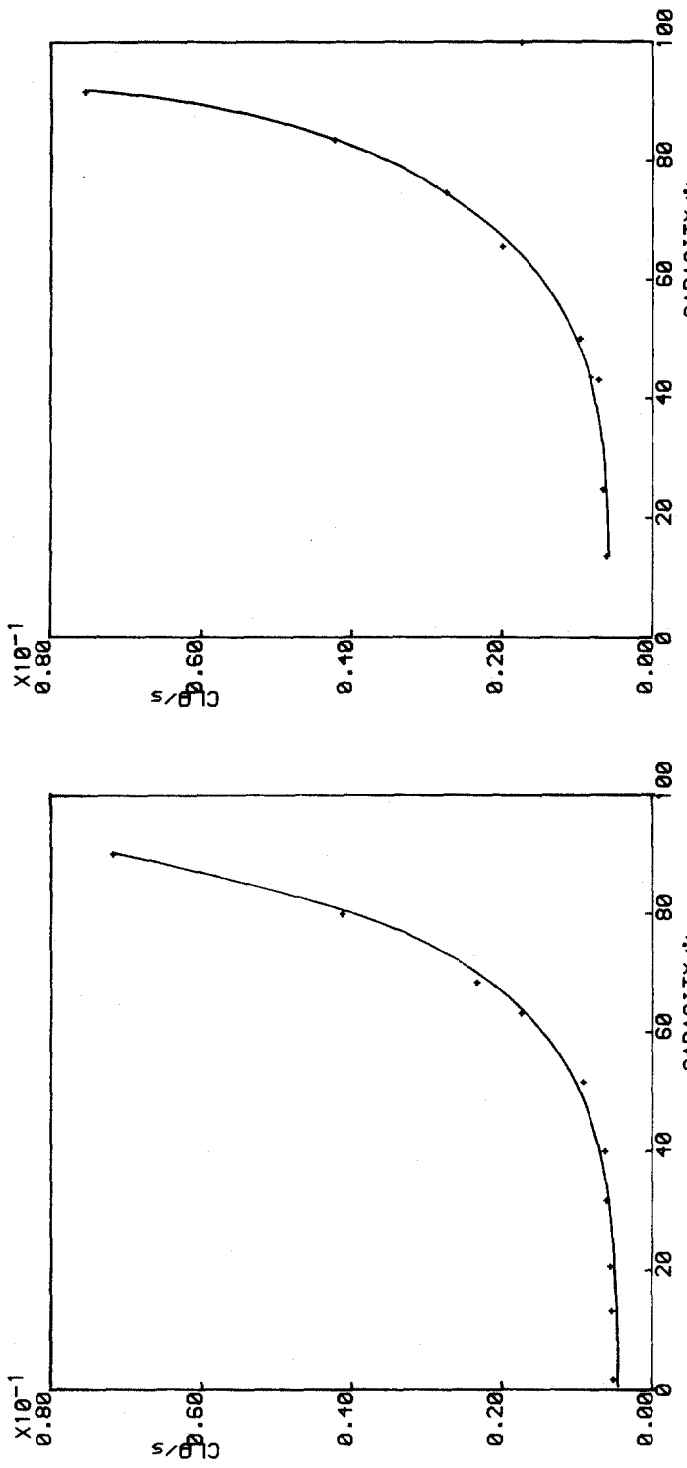

Fig. 22. Relationship between the product θC_L and the residual capacity of a new 25 A h cell discharged at the 1 C rate, from the data obtained using the analogue circuit shown in Fig. 15.

Fig. 23. Relationship between the product θC_L and the residual capacity of a new 25 A h cell discharged at the 2 C rate, from the data obtained using the analogue circuit shown in Fig. 15.

expected and reflects the reduction in the sulphuric acid concentration at reacting centres.

3. The identification of a residual capacity parameter

It was clear that, as in the case of the 2.5 A h cells [3], the components of the cell analogue did not change smoothly or consistently enough to provide a basis for a test. The argument developed earlier [3] for the 2.5 A h cells, in which we considered the product θC_L, where θ is the effective (experimental) charge-transfer resistance and C_L the effective experimental double-layer capacitance, was again considered in the case of these cells. Figures 22 - 25 show how the product θC_L varies with the residual capacity of both new and old cells discharged at the 1 and 2 C rates. The form of the relationship is identical with that for the 2.5 A h cells and shows the values of θC_L for each cell to be approximately independent of discharge rate.

Figures 26 - 29 show the product θC_L obtained at the maximum in the experimental impedance plotted against residual capacity for both new and old cells. Clearly, as before, the data provide an excellent estimation of the residual capacity in such cells in the 50 - 100% residual capacity range. Different cells provide similar shaped curves which extend over different ranges of $\theta' C_L$. This must reflect the differences in the material balance in the cells and clearly indicates the wide tolerances applied in their manufacture. In order that this test may be universally applied to these cells, improved tolerances would be necessary in their manufacture. This test can also be applied successfully to cells cycled hundreds of times and in commercial use.

Basic differences initially observed in the 2.5 A h cell [3] between differently aged and differently treated cells were not observed in the 25 A h cells. This suggests that in five years the old cell has not been cycled a sufficient number of times to cause noticeable wear on the positive plates.

The specific on-board residual capacity test for an aircraft battery, for example, cannot tolerate the necessity of a large amount of equipment inherent in our harmonic test procedure. We can now achieve a complete test via the isolation of the time constant in a few seconds using fast Fourier methods. These applications will be described in a later paper [8].

Conclusions

(i) The impedance spectrum of a lead–acid cell of relatively high capacity can yield useful information regarding the state-of-health of the cell.

(ii) The locus of the impedance (real *versus* imaginary) at high frequency always contains a "semicircle" representing charge-transfer resistance and double-layer capacitance.

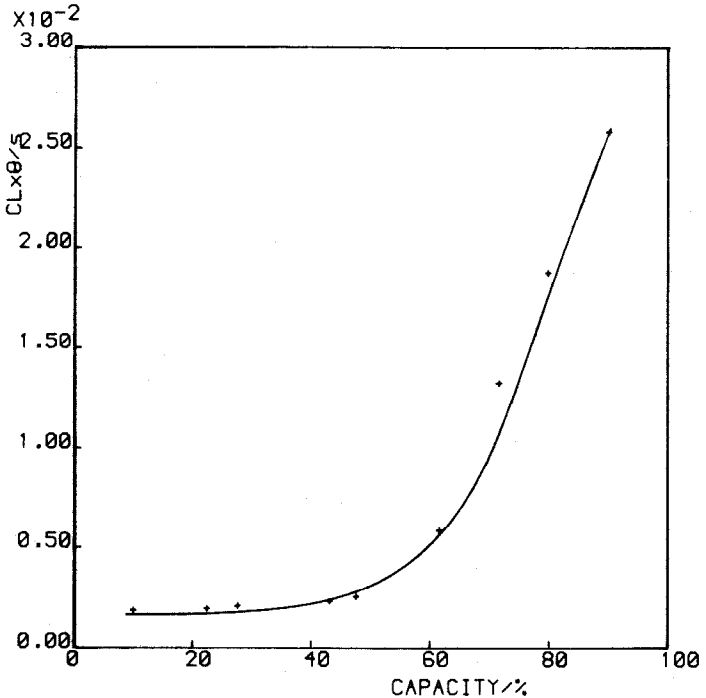

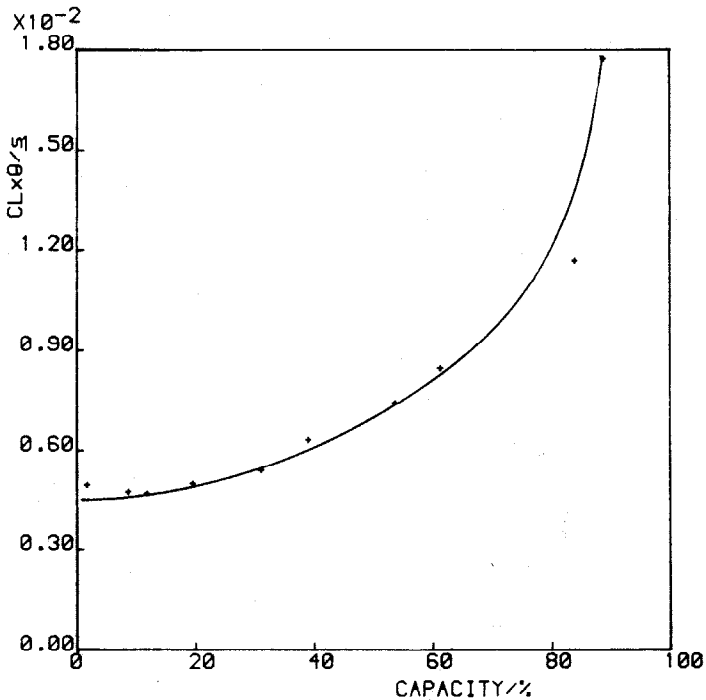

Fig. 24. Relationship between the product θC_L and the residual capacity of an old 25 A h cell discharged at the 1 C rate, from the data obtained using the analogue circuit shown in Fig. 15.

Fig. 25. Relationship between the product θC_L and the residual capacity of an old 25 A h cell discharged at the 2 C rate, from the data obtained using the analogue circuit shown in Fig. 15.

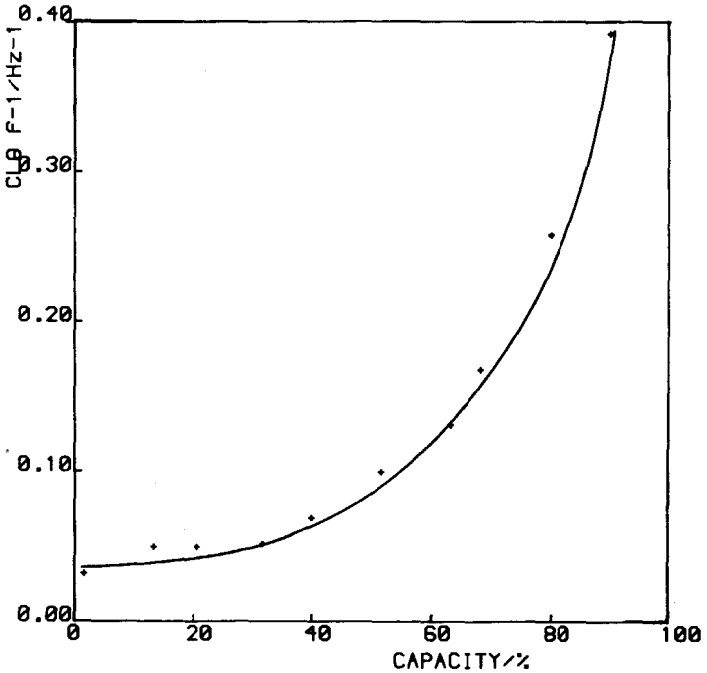

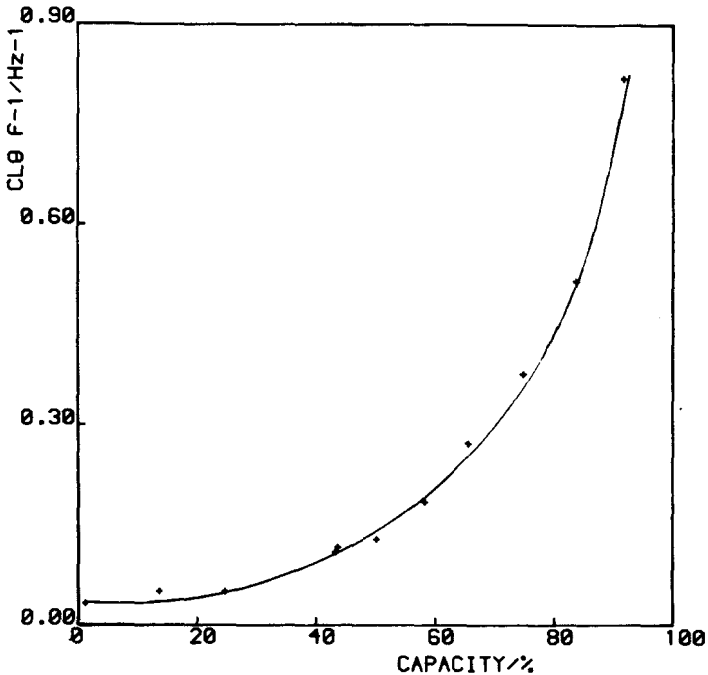

Fig. 26. Relationship between the product θC_L and the residual capacity for a new cell discharged at the 1 *C* rate but obtained directly from the experimental impedance from the reciprocal of the frequency at the top of the high frequency semicircle.

Fig. 27. Relationship between the product θC_L and the residual capacity for a new cell discharged at the 2 *C* rate but obtained directly from the experimental impedance from the reciprocal of the frequency at the top of the high frequency semicircle.

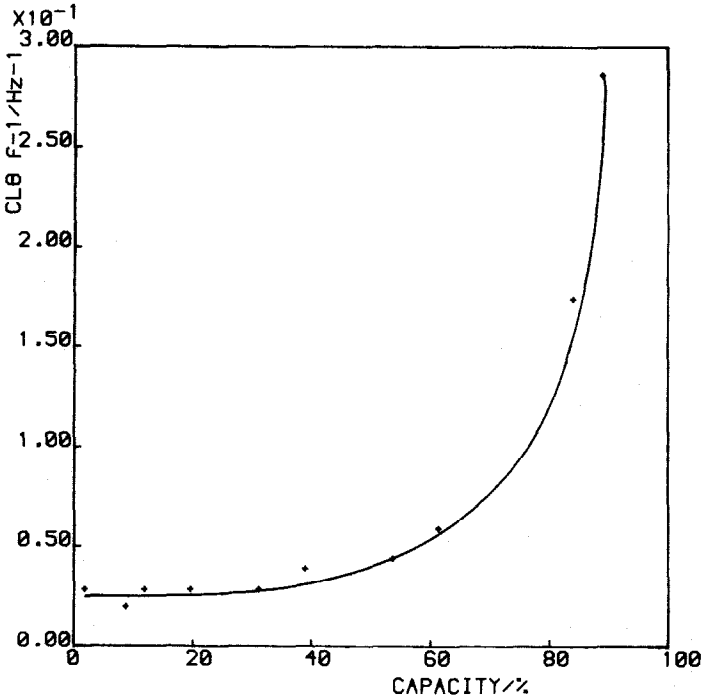

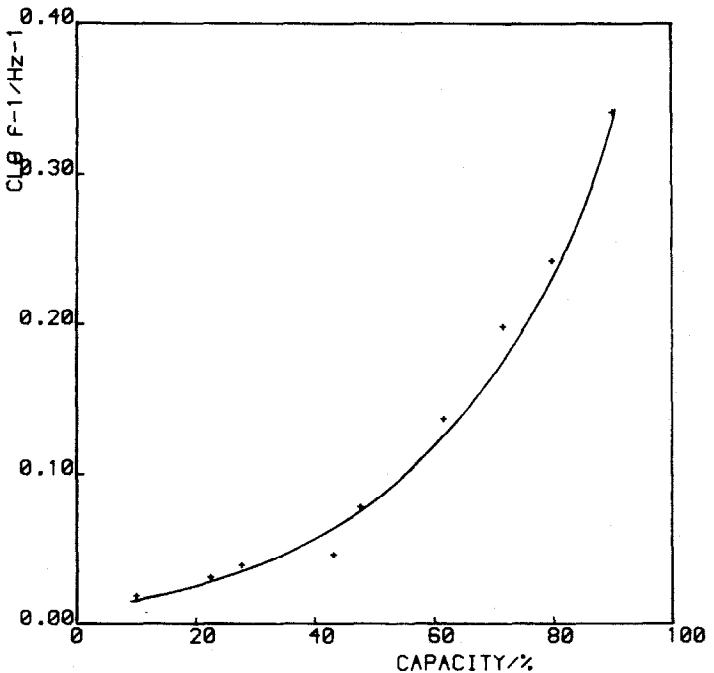

Fig. 28. Relationship between the product θC_L and the residual capacity for an old cell discharged at the 1 C rate but obtained directly from the experimental impedance from the reciprocal of the frequency at the top of the high frequency semicircle.

Fig. 29. Relationship between the product θC_L and the residual capacity for an old cell discharged at the 2 C rate but obtained directly from the experimental impedance from the reciprocal of the frequency at the top of the high frequency semicircle.

(iii) The time constant for this combination represented by the local maximum is a single-valued measure of the cell state-of-charge.

(iv) Further work on the other factors which contribute to these relationships is required: this is in hand.

Acknowledgement

This work was carried out with the support of Procurement Executive, Ministry of Defence.

References

1 M. Hughes, R. T. Barton, S. A. G. R. Karunathilaka, N. A. Hampson and R. Leek, *J. Appl. Electrochem.*, *15* (1985) 129.
2 S. A. G. R. Karunathilaka, R. T. Barton, M. Hughes and N. A. Hampson, *J. Appl. Electrochem.*, *15* (1985) 251.
3 M. Hughes, R. T. Barton, S. A. G. R. Karunathilaka and N. A. Hampson, *2nd Interim Report on the Pb/Acid Battery (Contract No. ER1A/9/4/2170/086XR/Mets Code No. CMB 189M)*, 2nd Nov. 1984; *J. Appl. Electrochem.*, in press.
4 Personal communication with R. F. Nelson, Technical Director, Gates Energy Products, Inc., Denver, Colorado.
5 M. Keddam, Z. Stoynov and H. Takenouti, *J. Appl. Electrochem.*, *7* (1977) 539.
6 E. Willinghanz, *J. Electrochem. Soc.*, *102* (1955) 599.
7 J. J. Lamden and E. E. Nelson, *J. Electrochem. Soc.*, *107* (1960) 723.
8 S. A. G. R. Karunathilaka and N. A. Hampson, *Int. J. Math. Educ. Sci. Technol.*, in press.